Strong influence of aerosol reductions on future heatwaves

Citation for published version:
Zhao, A, Bollasina, M & Stevenson, D 2019, 'Strong influence of aerosol reductions on future heatwaves', *Geophysical Research Letters*. https://doi.org/10.1029/2019GL082269

Digital Object Identifier (DOI):
10.1029/2019GL082269

Link:
Link to publication record in Edinburgh Research Explorer

Document Version:
Publisher's PDF, also known as Version of record

Published In:
Geophysical Research Letters

Zhao Alcide (Orcid ID: 0000-0002-8300-5872)
Bollasina Massimo (Orcid ID: 0000-0001-7509-7650)
Stevenson David, S (Orcid ID: 0000-0002-4745-5673)

Strong influence of aerosol reductions on future heatwaves

Alcide Zhao[1], Massimo A. Bollasina[1] and David S. Stevenson[1]

[1] School of GeoSciences, University of Edinburgh, Edinburgh, UK

Corresponding author: Alcide Zhao (alcide.zhao@ed.ac.uk)

Key Points:

- Future heatwaves will be more severe, primarily due to mean temperature increases, with minor impacts from temperature variability changes.
- Aerosol reductions will contribute most strongly to changes in heatwaves in the Northern Hemisphere extra-tropics.
- Per unit of warming, aerosol reductions, compared to greenhouse gases, lead to stronger heatwave responses via aerosol-cloud interactions.

Abstract

Using the Community Earth System Model Large Ensemble experiments, we investigate future heatwaves under the Representative Concentration Pathway 8.5 scenario, separating the relative roles of greenhouse gas increases and aerosol reductions. We show that there will be more severe heatwaves (in terms of intensity, duration and frequency) due to mean warming, with minor contributions from future temperature variability changes. While these changes come primarily from greenhouse gas (GHG) increases, aerosol reductions contribute significantly over the Northern Hemisphere. Furthermore, per degree of global warming, aerosol reductions induce a significantly stronger response in heatwave metrics relative to GHG increases. The stronger response to aerosols is associated with aerosol-cloud interactions which are still poorly understood and constrained in current climate models. This suggests that there may exist large uncertainties in future heatwave projections, highlighting the critical significance of reducing uncertainties in aerosol-cloud interactions for reliable projection of climate extremes and effective risk management.

Plain language summary

The past few years have seen record heatwaves worldwide, primarily driven by human activities. We used a state-of-the-art climate model to investigate future changes in heatwave characteristics under the Representative Concentration Pathway 8.5 scenario, and seek to separate the roles of projected changes in anthropogenic greenhouse gases and aerosols. The model shows that there will be more severe heatwaves (in terms of intensity, duration and frequency) primarily because of global warming, while the internal variability of the climate system does not change much by 2100 and hence has limited influences. Also, these changes are mainly associated with greenhouse gas increases. However, anthropogenic aerosol changes have important influences, through their effects on clouds and radiation, and produce larger impacts comparing to GHGs per unit of warming. Effects of aerosols on clouds such as changes in cloudiness and other rapid adjustments (e.g. changes in vertical temperature profiles), however, are still poorly represented in present generation climate models, leading to large uncertainties in future heatwave projections. Therefore, we call the attention of the community to prioritize efforts into reducing uncertainties involved in aerosol-cloud interactions, in order to get reliable projections of future climate extremes, as well as effective strategies for climate risk management.

1 Introduction

The increased frequency and severity of heatwaves under global warming has raised enormous public attention during the recent years, especially after the 2003 heatwave over Central and Western Europe (Bouchama, 2004; García-Herrera et al., 2010) that broke temperature records set over the last 500 years and led to more than 70,000 deaths and economic losses in excess of 13 billion euros (De Bono et al., 2004). The past few years have witnessed numerous heatwaves around the world reported as "record-breaking", "abnormal", "rare", and "catastrophic" by the media (Coumou and Rahmstorf, 2012; Russo et al., 2015; Ceccherini et al., 2017; Chen and Li, 2017). Under projected future climate warming, the intensity, frequency and duration of severe heatwaves are likely to increase further (Lau and Nath, 2014; Jones et al., 2015; Schoetter et al., 2015; Schär, 2016; Mora et al., 2017).

Heatwave changes can be exacerbated due to variations in many of their driving factors, including: climate variability and large-scale teleconnections, changes in circulations, land-atmosphere coupling, soil moisture feedbacks, and anthropogenic forcings (Brown et al., 2008; Field, 2012; Collins et al., 2013; Stott et al., 2013; Stocker, 2014; Perkins, 2015; Horton et al., 2016; Lu and Chen, 2016; Xu et al., 2016), with potential coupled feedbacks among them (Miralles et al., 2018). However, large gaps still remain in our understanding of the mechanisms underpinning changes in heatwaves, resulting in very uncertain future projections. For example, uncertainties in future emission pathways of anthropogenic forcing agents and the responses of climate models to them (Booth et al., 2013). Anthropogenic aerosols represent the largest uncertainty in radiative forcing since the pre-industrial times (Stevens and Feingold, 2009; Stocker, 2014; Stevens, 2017). A number of studies have shown that future aerosol reductions will lead to more severe temperature/heat extremes (Levy et al., 2013; Sillmann et al., 2013; Westervelt et al., 2015; Xu et al., 2015; Horton et al., 2016; Lin et al., 2016; Mascioli et al., 2016; Wang et al., 2016). However, the simplified temperature metrics used by these studies, such as the maximum of daily maximum temperature, do not necessarily represent heatwave characteristics (Chen and Li, 2017), because heatwaves are a quite distinctive type of temperature extreme where unusually hot weather occurs for several consecutive days.

Given that aerosol emissions are likely to reduce worldwide during the 21st century following stringent mitigation policies aimed at improving air quality, it is important to know the corresponding changes in heatwaves, as well as the relative roles of increasing greenhouse gases (GHGs) and decreasing aerosols at both global and regional scales, given their importance for policymaking and future climate risk management. Furthermore, since temperature variability may change along with climate change in the future (Schär et al., 2004), it is also critical to understand whether future changes in heatwaves will be more strongly driven by the mean temperature change or by changes in temperature variability, or a combination of both (Basarin et al., 2016). This study has three main aims: 1) to investigate future changes in the characteristics (intensity, duration, frequency and magnitude) of heatwaves at the global scale under the RCP8.5 scenario; 2) to compare the changes in heatwaves due to the shift of mean temperature and those related to changes in temperature variability; and 3) to quantify the relative roles of GHG increases and aerosol reductions. Methods used are described in Section 2, followed by results and discussion in Sections 3 and 4.

2 Methods

The Community Earth System Model Large Ensemble (CESM-LE) project (Kay et al., 2015) has two 1000+-yr-long preindustrial control simulations that allow us to quantify the internal climate variability. The 30 simulations of the 1920-2100 period can therefore be used to disentangle the signal of climate change from internal climate variability. The atmosphere component of CESM1 is the Community Atmosphere Model 5 (CAM5) (Conley et al., 2012), with a horizontal resolution of 0.9º x 1.25º. The ocean component has a resolution of 1º × 1º (Hurrell et al., 2013). In these simulations, atmospheric concentrations of well-mixed GHGs (e.g. CO_2 and CH_4) in CAM5 are prescribed. CAM5 includes a three-mode (Aitken, accumulation, and coarse) aerosol scheme (Modal Aerosol Mode 3). Several aerosol species (sulfate, organic carbon and black carbon, sea-salt, and dust) are simulated and their number concentrations and mass are prognostically calculated. Black carbon is emitted into the accumulation mode and ages, which allows it to be coated with soluble species (e.g., SO4) and to nucleate cloud droplets (Conley et al. 2012; Liu et al. 2012). In this study, we make use of two sets of CESM-LE experiments. The first set consists of a 30-member ensemble of historical (1920-2005) and future (2006-2100, following the RCP8.5 scenario) all-forcing simulations (Riahi et al., 2007; Van Vuuren et al., 2011). The RCP8.5 scenario shows global GHG increases and aerosol decreases, but with aerosol trends showing strong regional variations (see Figure S1 and Text S1). The second set is a 15-member ensemble of simulations that follow RCP8.5 for 2006-2100 but with fixed aerosol/precursor emissions at 2005 levels (hereinafter RCP8.5_FixA) (Lin et al., 2015; Xu et al., 2015). Each of the ensemble members has the same forcing and only differs with randomly perturbed initial atmospheric conditions (Kay et al., 2015).

The warming under scenario RCP8.5_FixA is primarily from GHG increases with minor contributions from factors such as land use changes (Xie et al., 2013; Shindell et al., 2015; Paul et al., 2016). For conciseness, we subsequently refer to changes under RCP8.5_FixA as GHG effects. Assuming that the response under RCP8.5 is a linear combination of GHGs and aerosols, the differences between RCP8.5 and RCP8.5_FixA then reflect the effects of aerosol changes (Zhao et al., 2018).

We focus on compound heatwave events (Chen and Li, 2017) which are identified as hot days persisting for at least 3 consecutive days at a land grid-box (see Text S2 and Figure S2 for more details). Hot days are defined as days when both daily maximum (TX) and minimum (TN) are greater than their 95th percentiles; these are derived over the 1961-1990 time period, using the 30 ensemble member simulations, and denoted as TX95P and TN95P respectively. To quantitatively describe the intensity and magnitude of heatwaves, we use the temperature excess above the 95th percentile threshold. The temperature excess for a specific heatwave day is defined as the mean of the differences (TX-TX95P) and (TN-TX95P) for each grid-box. Heatwaves are described by the following four metrics on an annual basis (Figure S2): (i) Maximum duration (the maximum duration of all heatwaves across a year); (ii) Peak intensity (the annual maximum heatwave intensity calculated as the average temperature excess throughout its duration); (iii) Frequency (the total number of heatwaves in a year); and (iv) Total hot days (the total includes both heatwave days and hot days that persist for less than three consecutive days).

In addition to the above four metrics, we use another index, the heatwave magnitude (see the caption of Figure S2). This index, calculated by summing temperature excesses throughout the duration of a heatwave (Russo and Sterl, 2011), has the advantage of merging duration and temperature excess into a single indicator, and is therefore indicative of the overall severity of a heatwave. Note that any heatwave metrics based on fixed (either absolute or percentile) thresholds may lose their effectiveness when the climate is warm enough. Also, we do not normalize heatwave magnitude metrics to avoid the possibility of misleading interpretations (Sippel et al., 2015). All metrics are calculated for each ensemble member for each year at each land point (excluding Antarctica). The ensemble mean and 25th-75th percentile spread of metrics are used in the following discussion. We also calculate, for each model land grid-box, the probability that future heatwave magnitudes will exceed their present-day local records (see Text S3 for more detail), following (Lehner et al., 2016). Note these probabilities can be biased as the CESM-LE members are not necessarily completely independent from each other.

To evaluate the performance of CESM-LE in simulating present-day (1986-2005) heatwaves characteristics, we also calculated the 1986-2005 heatwave using TX and TN from the National Centers for Environmental Prediction/National Center for Atmospheric Research reanalysis (Kalnay et al., 1996), as well as the Met Office Hadley Centre gridded daily temperatures (Caesar et al., 2006).

In order to diagnose the contribution of changes in future temperature variability to changes in heatwave characteristics, the above analysis is repeated after removing the decadal temperature trend from the raw temperature data at each grid-box. A 10-yr running mean of surface air temperature (see Figure S3) is first removed from both TX and TN to leave de-trended anomalies. New 95th percentile thresholds and heatwave metrics are then re-computed from the de-trended data.

3 Present-day and future projections of heatwave characteristics

We first show that CESM is able to reproduce observed heatwave characteristics, then investigate how changes in mean climate and climate variability drive future heatwave metric changes. We also isolate contributions to future change from GHG increases and aerosol reductions.

The performance of CESM-LE in capturing "present-day" heatwave metrics is evaluated comprehensively against two datasets (Figure S4-S5 and Text S4). Some parts of the world (e.g. Africa and S. America) lack observations; reanalysis data in these regions are also much more uncertain. CESM-LE can reasonably capture heatwave characteristics over most of the better-observed regions.

Figure 1a-d shows values of the four heatwave metrics for 'present-day' (1986-2005; green) and for two future (2081-2100) projections (blue: RCP8.5_FixA; red: RCP8.5), averaged at global scale as well as for specific regions (also see Figure s6). Corresponding spatial patterns of changes (future vs. present-day) in these metrics due to both GHG increases and aerosol reductions are provided in Figure S7. Figures 1a and S7a show that

GHG rises will increase global and regional mean annual peak heatwave intensities from ~2 K to ~4 K. Aerosol reductions further enhance heatwave intensities by about 0.3 K (Australia) to 0.7 K (Europe and China). The annual maximum heatwave duration shows future increases, from a present-day global mean value of 3.6 days, increasing to 21 days with GHG increases, and 28 days when aerosol reductions are also included. Heatwave duration shows strong regional variations, with the largest increases seen over Brazil (Figures 1b and S7b, f).

Changes in annual heatwave frequency (Figure 1c) and total hot days (Figure 1d) display similar features. Note, however, there is an exception of the heatwave frequency in Brazil (and also other tropical regions) that decreases as aerosols reduce (Figure S7g). This is because of the significantly longer heatwave durations.

By definition, temperature variability sets the baseline (1961-1990) values for the heatwave metrics, and that variability has changed little by 1986-2005, or by 2081-2100 (Figure 1e-h and S6e-h). This contrasts with the marked increases in metrics based upon absolute temperature changes, suggesting that future changes are largely associated with the general warming and only slightly modulated by temperature variability changes. Specifically, the relative contribution of temperature variability changes to the various heatwave metric changes is generally under 10% (Figure S8), except for heatwave intensity over Europe (24%), Brazil (21%) and India (11%) under both scenarios. In addition, the difference (Figure S8c) between RCP8.5 and RCP8.5_FixA suggests that future aerosol reductions will generally decrease the contribution of changes in temperature variability. This is particularly true for heatwave duration: a reduction ranging from a global mean of -0.5 % to a regional peak of -2.5% over Australia. This suggests that aerosol reductions will slightly dampen temperature variability in the future (see further discussions in Section 4).

We also analyzed data by season, but found only small seasonal signals. We found that there will be slightly stronger changes in summertime heatwaves compared to wintertime, and that the seasonal contrast was amplified by aerosol reductions. See Text S6 and Table S1, S2 for more details.

In summary, future GHG increases will result in future (2081-2100) heatwaves that are, when globally averaged over land, significantly more intense (2.4 K), longer (17 days), and more frequent (12 more per year), compared to present-day. These changes will be further aggravated by aerosol reductions. Namely, 0.6 K (25%), 7 days (41%) and 2 more per year (12%) of additional increases in intensity, duration and frequency, respectively, on top those related to GHG changes. Changes to heatwaves are similar in all seasons, and are dominated by changes in mean temperature, with only minor contributions from changes in temperature variability.

4 Probabilities of record future heatwaves and driving mechanisms

We now turn our attention to the heatwave magnitude metric, and examine the probability that present-day heatwave magnitudes will be exceeded in future. As above, we use the two scenarios to isolate the roles of GHG increases and aerosol decreases.

4.1 Exceedance probability of future heatwave magnitude over present-day record

Under the RCP8.5 scenario, the tropics see earlier emergences of heatwave magnitudes exceeding their 1986-2005 records (Figure 2a). Further, the exceedance probability is much larger over the tropics than at higher latitudes during both time periods. An explanation is that the relatively small temperature variability in the tropics makes it easier to break the historical record with relatively small increases in mean temperature compared to higher latitudes. This agrees with existing works showing that the tropics will see the earliest emergence of significant warming (Mahlstein et al., 2011; Lehner et al., 2016). By 2081-2100, almost every year will have record-breaking heatwaves, with a global mean exceedance probability of 76% (Figure 2b). Not surprisingly, under the fixed aerosol scenario (Figure 2c,d), the probability is significantly smaller over the NH, where most aerosols are emitted. For aerosols (Figure 2e,f), although there are some signals in the SH, probability changes here are primarily associated with GHG increases (Figure 2c, d). In contrast, the aerosol signal is mainly over the NH. For example, aerosol reductions will increase the exceedance probability by a further 20%, on top of a 52% increase due to GHGs in Europe by 2081-2100.

4.2 Sensitivity of heatwaves to warming mechanism

As both GHG increases and aerosol reductions result in future warming, one may ask whether changes in heatwaves are more sensitive to one or the other. This is important because the sensitivities can be useful to assess the impacts of different future mitigation strategies. Here we examine the sensitivity of future changes in heatwave metrics per unit of global land warming. The sensitivities are calculated as the slope of the linear fit between annual mean heatwave metrics and global land mean temperature changes (Figure 3a-c). Note the fitting was performed for 2041-2060 and 2081-2100 (Figure 3d-f) separately since these metrics increase exponentially with warming. The time evolution of these metrics together with other variables used to examine the driving mechanisms of such changes are provided in Figure S9.

Heatwave intensity scales relatively linearly with warming from both GHG increases and aerosol reductions (Figure 3a), yet the latter leads to a greater heatwave intensity increase than the former per unit of warming over both the two time periods (Figure 3d). In fact, the larger sensitivity to warming from aerosol reductions (as compared to GHG increases) stands for all the three heatwave metrics during both time periods (Figure 3d-f). In the following we focus on the time period 2081-2100 unless otherwise stated. Over the period 2081-2100, surface mean temperature changes related to aerosol changes (diagnosed as the difference between RCP8.5 and RCP8.5_FixA, see Figure S9a) tend to stabilize at around 0.8K. However, over the same time period, heatwave duration related to aerosols continue to rise from ~ 1.2 days in 2080 to 1.8 days by 2100. (Figure S9e). As a consequence, the sensitivity of heatwave duration to warming from aerosol reductions 2 times of that warming from GHG increases. Aerosol reductions result in changes in heatwave intensity (Figures 3a, S9d) and duration (Figures 3b, S9e), in combination (but mainly due to changes in duration), lead the heatwave magnitude to increase exponentially with warming (Figure 3c). This leads to an even larger (2.4 times that of GHG increases) sensitivity of heatwave magnitude to warming from aerosol reductions (Figure 3f).

The steepest parts of the aerosol-related curves in Figure 3a-c correspond to the time period when the aerosols are sufficiently low in the atmosphere (i.e. late 21st century in the RCP8.5 scenario), continuing aerosol reductions tend not to change mean temperature but increase heatwave magnitude exponentially. Because heatwaves are defined using TX and TN, we examine if the larger sensitivity to aerosol reductions discussed above stems from changes in maximum (Figure 3g) and/or minimum (Figure 3j) temperatures. It can be seen aerosol reductions induced exponential TX changes that resemble the shape of the heatwave duration/magnitude relationship with surface temperature, while TN increases linearly with warming. Therefore, it is the changes in TX that lead to dramatic increases in heatwave magnitude. This is particularly important over regions of the largest emission sources such as China, Europe, USA and. India (Figure S10).

We further investigate if this is related to aerosol direct and/or indirect effects, by examining representative aerosol effect indicators: cloud liquid water path (CLWP, Figure 3h), shortwave cloud forcing (SWCF, Figure 3i) clear-sky shortwave radiation at top-of-the-atmosphere (SWCST in Figure 3k), as well as longwave cloud forcing (LWCF, Figure 3l) cloud forcing. Note that although cloud can be influenced by dynamic and thermodynamic processes (Rosenfeld et al., 2008; Yu et al., 2014), the strong linear correlation between changes in AOD and cloud forcing (an R^2 of 0.93 for SWCF and 0.80 for LWCF) (Figure S11) demonstrates that the aerosol-induced changes in cloud microphysics are the main drivers of the additional cloud forcing changes. Clearly, when the aerosol reductions resulted in little change in mean warming in 2081-2100, both CLWP (Figure 3h) and SWCF (Figure 3i) show dramatic changes that significantly deviate from their linear correlations with warming during 2006-2081. In contrast, SWCST and LWCF continue to show a linear correlation with temperature changes that does not differ much between GHG increases and aerosol reductions (Figures 3k, l). Overall, these indicate the importance of aerosol-cloud interactions rather than the aerosol direct effect in increasing TX and thereby heatwave duration/magnitude in a dramatic way. Specifically, when aerosol loading is low by 2081-2100, mean temperature and TN tend to stabilize (Figure S9a, b). However, TX increases exponentially (Figures 3i, S9c), because of large changes in aerosol-cloud interactions.

We speculate that the exponential increases in TX and heatwave magnitude/duration due to aerosol-cloud interactions is related to the exponential relationship between aerosol radiative forcing, cloud microphysics and aerosol loading as discussed by Wilcox et al. (2015). More specifically, when the aerosol loadings are sufficiently low, small changes in aerosols can lead to significantly larger responses in cloud droplet size and cloud albedo, compared to the behaviour when the aerosol loadings are high. These result in exponential increases in shortwave radiation reaching the surface (Figure 3i) during daytime as well as a more unstable daytime atmosphere (because cloud lifetime and amount reduce as droplet size increases). Therefore, daytime temperatures increase and become more variable while the nighttime temperatures are less influenced by aerosol-cloud interactions. Consequently, unlike mean temperature and TN, TX continues to increase.

Finally, for the same amount of mean warming, TX and heatwave duration increase dramatically due to aerosol reductions (Figure 3b, e), but this does not occur in the case of GHG increases. This suggests that aerosol reductions dampen the day-to-day TX variability. That is, the more variable the TX is from day to day, the fewer the consecutive days with TX above TX95P, and vice versa. The dampening of temperature variability from aerosols reductions, by reducing the chances of intermittent cool days, would lead us to suffer more from persistent heatwaves. A physical explanation is that aerosol reductions may contract the Hadley cell (Allen and Sherwood, 2011) and shift the NH Hadley branch and jet stream northward (Lucas et al., 2014; Rotstayn et al., 2014; Xu and Xie, 2015; Chemke and Dagan, 2018). In combination these effects dampen atmospheric variability over the tropics and extra-tropics.

5 Discussion and conclusions

A large body of literature has suggested that future GHG increases will very likely enhance the duration, intensity and frequency of heat extremes across the world (Meehl and Tebaldi, 2004; Lau and Nath, 2014; Russo et al., 2014; Jones et al., 2015; Schoetter et al., 2015; Schär, 2016; Mishra et al., 2017; Mora et al., 2017). However, very little attention has been devoted to contrasting the roles of future GHG increases and aerosol reductions in future heatwave characteristic projections. A few studies have linked future aerosol reductions and increased temperature (or heat) extremes (Xu et al., 2015; Horton et al., 2016). However, their findings did not account for the duration of extreme temperature events, which is critical to properly characterizing a heatwave.

In this study, we make use of the CESM-LE to investigate the effects of both GHGs and aerosols on changes in heatwave characteristics in the future. We show that all the heatwave metrics—intensity, duration, frequency, total hot days and magnitude -- increase during the 21st century, primarily in response to the long-term warming and with a minor contribution from future temperature variability changes. Note that these heatwave metrics are influenced by the local temperature variability, and should be used in combination to interpret more fully the characteristics of heatwaves. In addition, GHG increases will account for most of these changes while aerosol reductions will exert their impact especially over the NH. However, given the same amount of warming, aerosol reductions are shown to increase the heatwave magnitudes in highly non-linear ways, through aerosol-cloud interactions. The various RCP scenarios have similar aerosol—but different GHG—emission pathways (Lamarque et al., 2013). In particular, the lower GHG increases in other RCP scenarios compared to RCP8.5 may induce smaller changes in heatwave metrics. Therefore, aerosols are likely to play a more important role in future heatwave projections. Furthermore, these heatwave metrics may differ under other future scenarios such as the shared socio-economic pathways in which the spatial patterns of emission reductions differ (Gidden et al., 2018).

The overall minor contribution of changes in temperature variability to future heatwave changes indicates the importance of the choice of the baseline (1961-1990 in this case) in setting the threshold for identifying the occurrence of a heatwave. In addition, “present-day” is defined as 1986-2005. Choosing a later period (1996-2015) result in only very minor changes, and does not influence the conclusions. We acknowledge that our analysis is based on one model, and it is currently unknown if the projections of changes in heatwave metrics described here hold across models. Climate models represent background aerosols differently (Carslaw et al., 2013); these may lead to differences in the magnitude of forced response to changing aerosols between models. This is particularly important in an already aerosol-limited environment (Samset, 2018; Lewinschal et al., 2019), and may suggest that the non-linear responses in heatwave metrics to aerosol changes are model dependent. Therefore, further research, using similar methods, is needed to further assess our findings.

To summarize, the CESM model indicates that major changes in anthropogenic aerosols over the coming century can have very significant impacts on future heatwaves through aerosol-cloud interactions. However, the caveat is that this might only be a reflection of the specific aerosol scheme in CESM. In fact, there still are large uncertainties in our understanding of aerosol-cloud-radiation interactions, leading to poorly-constrained and diverging aerosol schemes in present generation climate models (Wilcox et al., 2015; Lee et al., 2016; Seinfeld et al., 2016; Malavelle et al., 2017). Therefore, our present projection of future heatwaves, and perhaps other types of climate extremes, might have large uncertainties. However, given the detrimental impacts of changes in future heatwaves and to more effectively manage climate risks, we call the attention of the community to prioritize efforts in reducing uncertainties in aerosol-cloud-radiation interactions.

Acknowledgement Alcide Zhao was jointly funded by the University of Edinburgh and the China Scholarships Council. M. A. Bollasina was supported by the UK-China Research and Innovation Partnership Fund through the Met Office Climate Science for Service Partnership (CSSP) China as part of the Newton Fund. D. S. Stevenson acknowledges support from NERC grant NE/N003411/1. The authors acknowledge the use of datasets from Met Office Hadley Centre and NCEP/NCAR. We thank the Community Earth System Model project at the National Centre for Atmosphere Research (NCAR) and the use of the UK National Supercomputing Service ARCHER. We thank Leighton Regayre and the other anonymous reviewer for their very constructive and valuable comments. All heatwave metrics, freely available on https://doi.org/10.5281/zenodo.2593585, are calculated using the CESM-LENS dataset which can be downloaded from the climate data gateway at NCAR.

References

Allen, R. J., and S. C. Sherwood (2011), The impact of natural versus anthropogenic aerosols on atmospheric circulation in the Community Atmosphere Model, Climate dynamics, 36(9-10), 1959-1978.

Basarin, B., T. Lukić, and A. Matzarakis (2016), Quantification and assessment of heat and cold waves in Novi Sad, Northern Serbia, International journal of biometeorology, 60(1), 139-150.

Booth, B., D. Bernie, D. McNeall, E. Hawkins, J. Caesar, C. Boulton, P. Friedlingstein, and D. Sexton (2013), Scenario and modelling uncertainty in global mean temperature change derived from emission-driven global climate models, Earth System Dynamics, 4(1), 95-108.

Bouchama, A. (2004), The 2003 European heat wave, Intensive care medicine, 30(1), 1-3.

Brown, S., J. Caesar, and C. A. Ferro (2008), Global changes in extreme daily temperature since 1950, Journal of Geophysical Research: Atmospheres, 113(D5).

Caesar, J., L. Alexander, and R. Vose (2006), Large-scale changes in observed daily maximum and minimum temperatures: Creation and analysis of a new gridded data set, Journal of Geophysical Research: Atmospheres, 111(D5).

Carslaw, K., L. Lee, C. Reddington, K. Pringle, A. Rap, P. Forster, G. Mann, D. Spracklen, M. Woodhouse, and L. Regayre (2013), Large contribution of natural aerosols to uncertainty in indirect forcing, Nature, 503(7474), 67.

Ceccherini, G., S. Russo, I. Ameztoy, A. F. Marchese, and C. Carmona-Moreno (2017), Heat waves in Africa 1981-2015, observations and reanalysis, Natural Hazards and Earth System Sciences, 17(1), 115.

Chemke, R., and G. Dagan (2018), The effects of the spatial distribution of direct anthropogenic aerosols radiative forcing on atmospheric circulation, Journal of Climate, 31(17), 7129-7145.

Chen, Y., and Y. Li (2017), An Inter-comparison of Three Heat Wave Types in China during 1961–2010: Observed Basic Features and Linear Trends, Scientific Reports, 7, 45619.

Collins, M., R. Knutti, J. Arblaster, J.-L. Dufresne, T. Fichefet, P. Friedlingstein, X. Gao, W. Gutowski, T. Johns, and G. Krinner (2013), Long-term climate change: projections, commitments and irreversibility.

Conley, A. J., R. Garcia, D. Kinnison, J.-F. Lamarque, D. Marsh, M. Mills, A. K. Smith, S. Tilmes, F. Vitt, and H. Morrison (2012), Description of the NCAR community atmosphere model (CAM 5.0), NCAR technical note.

Coumou, D., and S. Rahmstorf (2012), A decade of weather extremes, Nature climate change, 2(7), 491-496.

De Bono, A., P. Peduzzi, S. Kluser, and G. Giuliani (2004), Impacts of summer 2003 heat wave in Europe.

Field, C. B. (2012), Managing the risks of extreme events and disasters to advance climate change adaptation: special report of the intergovernmental panel on climate change, Cambridge University Press.

García-Herrera, R., J. Díaz, R. M. Trigo, J. Luterbacher, and E. M. Fischer (2010), A review of the European summer heat wave of 2003, Critical Reviews in Environmental Science and Technology, 40(4), 267-306.

Gidden, M., K. Riahi, S. Smith, S. Fujimori, G. Luderer, E. Kriegler, D. P. van Vuuren, M. van den Berg, L. Feng, and D. Klein (2018), Global emissions pathways under different socioeconomic scenarios for use in CMIP6: a dataset of harmonized emissions trajectories through the end of the century, Geoscientific Model Development Discussions, 1-42.

Horton, R. M., J. S. Mankin, C. Lesk, E. Coffel, and C. Raymond (2016), A review of recent advances in research on extreme heat events, Current Climate Change Reports, 2(4), 242-259.

Hurrell, J. W., M. M. Holland, P. R. Gent, S. Ghan, J. E. Kay, P. J. Kushner, J.-F. Lamarque, W. G. Large, D. Lawrence, and K. Lindsay (2013), The community earth system model: a framework for collaborative research, Bulletin of the American Meteorological Society, 94(9), 1339-1360.

Jones, B., B. C. O'Neill, L. McDaniel, S. McGinnis, L. O. Mearns, and C. Tebaldi (2015), Future population exposure to US heat extremes, Nature Climate Change, 5(7), 652.

Kalnay, E., M. Kanamitsu, R. Kistler, W. Collins, D. Deaven, L. Gandin, M. Iredell, S. Saha, G. White, and J. Woollen (1996), The NCEP/NCAR 40-year reanalysis project, Bulletin of the American meteorological Society, 77(3), 437-471.

Kay, J., C. Deser, A. Phillips, A. Mai, C. Hannay, G. Strand, J. Arblaster, S. Bates, G. Danabasoglu, and J. Edwards (2015), The Community Earth System Model (CESM) large ensemble project: A community resource for studying climate change in the presence of internal climate variability, Bulletin of the American Meteorological Society, 96(8), 1333-1349.

Lamarque, J.-F., D. T. Shindell, B. Josse, P. Young, I. Cionni, V. Eyring, D. Bergmann, P. Cameron-Smith, W. J. Collins, and R. Doherty (2013), The Atmospheric Chemistry and Climate Model Intercomparison Project (ACCMIP): overview and description of models, simulations and climate diagnostics, Geoscientific Model Development, 6(1), 179-206.

Lau, N.-C., and M. J. Nath (2014), Model simulation and projection of European heat waves in present-day and future climates, Journal of Climate, 27(10), 3713-3730.

Lee, L. A., C. L. Reddington, and K. S. Carslaw (2016), On the relationship between aerosol model uncertainty and radiative forcing uncertainty, Proceedings of the National Academy of Sciences, 113(21), 5820-5827.

Lehner, F., C. Deser, and B. M. Sanderson (2016), Future risk of record-breaking summer temperatures and its mitigation, Climatic Change, 1-13.

Levy, H., L. W. Horowitz, M. D. Schwarzkopf, Y. Ming, J. C. Golaz, V. Naik, and V. Ramaswamy (2013), The roles of aerosol direct and indirect effects in past and future climate change, Journal of Geophysical Research: Atmospheres, 118(10), 4521-4532.

Lewinschal, A., A. M. Ekman, H.-C. Hansson, M. Sand, T. K. Berntsen, and J. Langner (2019), Local and remote temperature response of regional SO 2 emissions, Atmospheric Chemistry and Physics, 19(4), 2385-2403.

Lin, L., A. Gettelman, Q. Fu, and Y. Xu (2015), Simulated differences in 21st century aridity due to different scenarios of greenhouse gases and aerosols, Climatic Change, 1-16.

Lin, L., Z. Wang, Y. Xu, and Q. Fu (2016), Sensitivity of precipitation extremes to radiative forcing of greenhouse gases and aerosols, Geophysical Research Letters, 43(18), 9860-9868.

Lu, R.-Y., and R.-D. Chen (2016), A review of recent studies on extreme heat in China, Atmospheric and Oceanic Science Letters, 9(2), 114-121.

Lucas, C., B. Timbal, and H. Nguyen (2014), The expanding tropics: A critical assessment of the observational and modeling studies, Wiley Interdisciplinary Reviews: Climate Change, 5(1), 89-112.

Mahlstein, I., R. Knutti, S. Solomon, and R. Portmann (2011), Early onset of significant local warming in low latitude countries, Environmental Research Letters, 6(3), 034009.

Malavelle, F. F., J. M. Haywood, A. Jones, A. Gettelman, L. Clarisse, S. Bauduin, R. P. Allan, I. H. H. Karset, J. E. Kristjánsson, and L. Oreopoulos (2017), Strong constraints on aerosol–cloud interactions from volcanic eruptions, Nature, 546(7659), 485.

Mascioli, N. R., A. M. Fiore, M. Previdi, and G. Correa (2016), Temperature and Precipitation Extremes in the United States: Quantifying the Responses to Anthropogenic Aerosols and Greenhouse Gases,+, Journal of Climate, 29(7), 2689-2701.

Meehl, G. A., and C. Tebaldi (2004), More intense, more frequent, and longer lasting heat waves in the 21st century, Science, 305(5686), 994-997.

Miralles, D. G., P. Gentine, S. I. Seneviratne, and A. J. Teuling (2018), Land–atmospheric feedbacks during droughts and heatwaves: state of the science and current challenges, Annals of the New York Academy of Sciences.

Mishra, V., S. Mukherjee, R. Kumar, and D. A. Stone (2017), Heat wave exposure in India in current, 1.5° C, and 2.0° C worlds, Environmental Research Letters, 12(12), 124012.

Mora, C., B. Dousset, I. R. Caldwell, F. E. Powell, R. C. Geronimo, C. R. Bielecki, C. W. Counsell, B. S. Dietrich, E. T. Johnston, and L. V. Louis (2017), Global risk of deadly heat, Nature Climate Change, 7(7), 501.

Paul, S., S. Ghosh, R. Oglesby, A. Pathak, A. Chandrasekharan, and R. Ramsankaran (2016), Weakening of Indian summer monsoon rainfall due to changes in land use land cover, Scientific Reports, 6, 32177.

Perkins, S. E. (2015), A review on the scientific understanding of heatwaves—their measurement, driving mechanisms, and changes at the global scale, Atmospheric Research, 164, 242-267.

Riahi, K., A. Grübler, and N. Nakicenovic (2007), Scenarios of long-term socio-economic and environmental development under climate stabilization, Technological Forecasting and Social Change, 74(7), 887-935.

Rosenfeld, D., U. Lohmann, G. B. Raga, C. D. O'Dowd, M. Kulmala, S. Fuzzi, A. Reissell, and M. O. Andreae (2008), Flood or drought: how do aerosols affect precipitation?, science, 321(5894), 1309-1313.

Rotstayn, L. D., E. L. Plymin, M. A. Collier, O. Boucher, J.-L. Dufresne, J.-J. Luo, K. von Salzen, S. J. Jeffrey, M.-A. Foujols, and Y. Ming (2014), Declining aerosols in CMIP5 projections: Effects on atmospheric temperature structure and midlatitude jets, Journal of Climate, 27(18), 6960-6977.

Russo, S., and A. Sterl (2011), Global changes in indices describing moderate temperature extremes from the daily output of a climate model, Journal of Geophysical Research: Atmospheres, 116(D3).

Russo, S., J. Sillmann, and E. M. Fischer (2015), Top ten European heatwaves since 1950 and their occurrence in the coming decades, Environmental Research Letters, 10(12), 124003.

Russo, S., A. Dosio, R. G. Graversen, J. Sillmann, H. Carrao, M. B. Dunbar, A. Singleton, P. Montagna, P. Barbola, and J. V. Vogt (2014), Magnitude of extreme heat waves in present climate and their projection in a warming world, Journal of Geophysical Research: Atmospheres, 119(22).

Samset, B. H. (2018), How cleaner air changes the climate, Science, 360(6385), 148-150.

Schär, C. (2016), Climate extremes: the worst heat waves to come, Nature Climate Change, 6(2), 128.

Schär, C., P. L. Vidale, D. Lüthi, C. Frei, C. Häberli, M. A. Liniger, and C. Appenzeller (2004), The role of increasing temperature variability in European summer heatwaves, Nature, 427(6972), 332.

Schoetter, R., J. Cattiaux, and H. Douville (2015), Changes of western European heat wave characteristics projected by the CMIP5 ensemble, Climate dynamics, 45(5-6), 1601-1616.

Seinfeld, J. H., C. Bretherton, K. S. Carslaw, H. Coe, P. J. DeMott, E. J. Dunlea, G. Feingold, S. Ghan, A. B. Guenther, and R. Kahn (2016), Improving our fundamental understanding of the role of aerosol− cloud interactions in the climate system, Proceedings of the National Academy of Sciences, 113(21), 5781-5790.

Shindell, D., G. Faluvegi, L. Rotstayn, and G. Milly (2015), Spatial patterns of radiative forcing and surface temperature response, Journal of Geophysical Research: Atmospheres, 120(11), 5385-5403.

Sillmann, J., L. Pozzoli, E. Vignati, S. Kloster, and J. Feichter (2013), Aerosol effect on climate extremes in Europe under different future scenarios, Geophysical Research Letters, 40(10), 2290-2295.

Sippel, S., J. Zscheischler, M. Heimann, F. E. Otto, J. Peters, and M. D. Mahecha (2015), Quantifying changes in climate variability and extremes: Pitfalls and their overcoming, Geophysical Research Letters, 42(22), 9990-9998.

Stevens, B. (2017), Climate science: Clouds unfazed by haze, Nature, 546(7659), 483.

Stevens, B., and G. Feingold (2009), Untangling aerosol effects on clouds and precipitation in a buffered system, Nature, 461(7264), 607.

Stocker (2014), Climate change 2013: the physical science basis: Working Group I contribution to the Fifth assessment report of the Intergovernmental Panel on Climate Change, Cambridge University Press.

Stott, P. A., M. Allen, N. Christidis, R. M. Dole, M. Hoerling, C. Huntingford, P. Pall, J. Perlwitz, and D. Stone (2013), Attribution of weather and climate-related events, in Climate Science for Serving Society, edited, pp. 307-337, Springer.

Van Vuuren, D. P., J. Edmonds, M. Kainuma, K. Riahi, A. Thomson, K. Hibbard, G. C. Hurtt, T. Kram, V. Krey, and J.-F. Lamarque (2011), The representative concentration pathways: an overview, Climatic change, 109(1-2), 5.

Wang, Z., L. Lin, M. Yang, and Y. Xu (2016), The effect of future reduction in aerosol emissions on climate extremes in China, Climate Dynamics, 1-15.

Westervelt, D., L. Horowitz, V. Naik, J.-C. Golaz, and D. Mauzerall (2015), Radiative forcing and climate response to projected 21st century aerosol decreases, Atmospheric Chemistry and Physics, 15(22), 12681-12703.

Wilcox, L., E. Highwood, B. Booth, and K. Carslaw (2015), Quantifying sources of inter-model diversity in the cloud albedo effect, Geophysical Research Letters, 42(5), 1568-1575.

Xie, S.-P., B. Lu, and B. Xiang (2013), Similar spatial patterns of climate responses to aerosol and greenhouse gas changes, Nature Geoscience, 6(10), 828-832.

Xu, Y., and S.-P. Xie (2015), Ocean mediation of tropospheric response to reflecting and absorbing aerosols, Atmospheric Chemistry and Physics, 15(10), 5827-5833.

Xu, Y., J.-F. Lamarque, and B. M. Sanderson (2015), The importance of aerosol scenarios in projections of future heat extremes, Climatic Change, 1-14.

Xu, Z., G. FitzGerald, Y. Guo, B. Jalaludin, and S. Tong (2016), Impact of heatwave on mortality under different heatwave definitions: a systematic review and meta-analysis, Environment international, 89, 193-203.

Yu, S., K. Alapaty, R. Mathur, J. Pleim, Y. Zhang, C. Nolte, B. Eder, K. Foley, and T. Nagashima (2014), Attribution of the United States “warming hole”: Aerosol indirect effect and precipitable water vapor, Scientific reports, 4, 6929.

Zhao, A. D., D. S. Stevenson, and M. A. Bollasina (2018), The role of anthropogenic aerosols in future precipitation extremes over the Asian Monsoon Region, Climate Dynamics, 1-22.

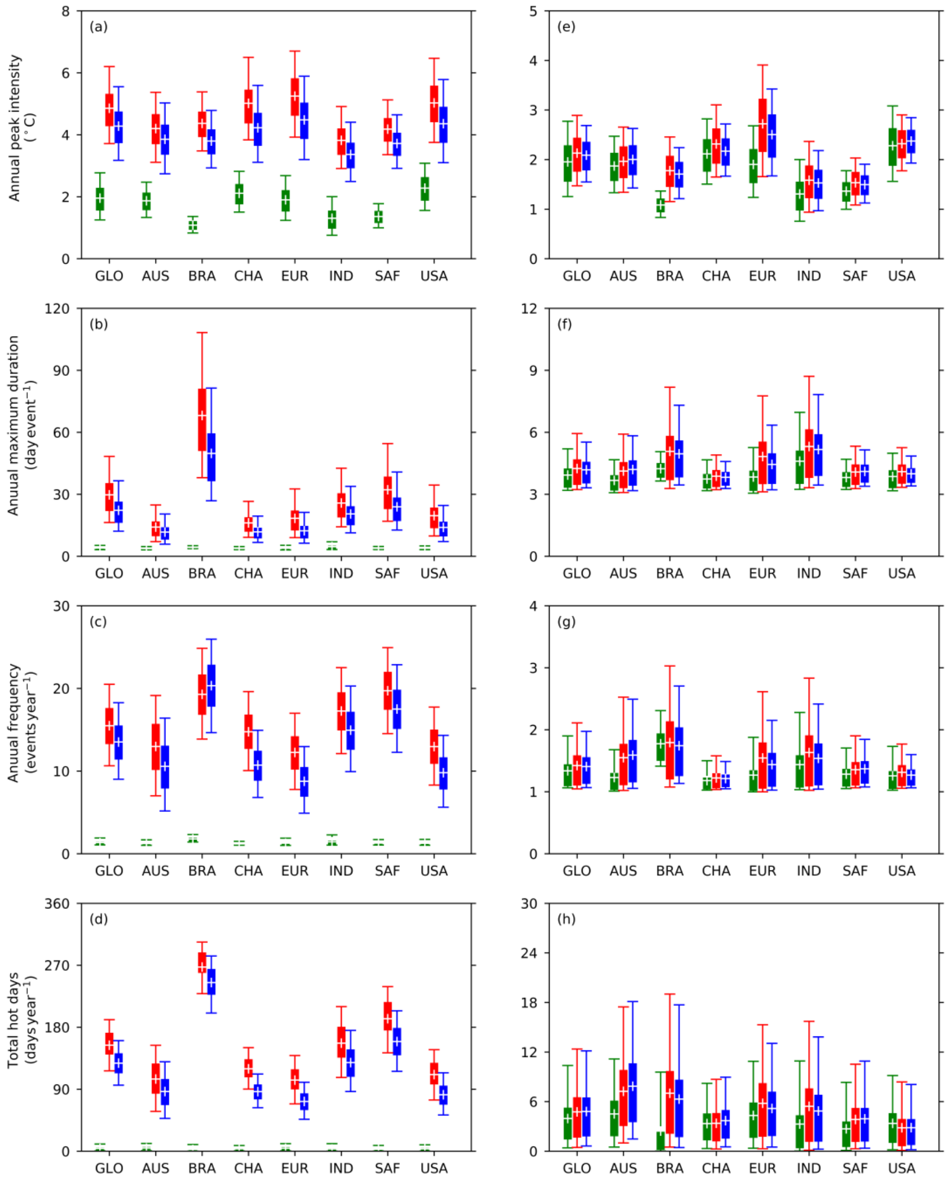

Figure 1 Area-weighted mean of twenty years mean of ensemble mean (white cross), 25th – 75th percentile spread (box), as well as ensemble minimum and maximum (whiskers) of heatwave metrics: (**a**) annual peak intensity (K), (**b**) annual maximum duration (days event^{-1}), (**c**) annual frequency (number year^{-1}) and (**d**) annual total days (days year^{-1}), derived from the absolute temperatures. Green for the period 1986-2005, red for 2081-2100 under RCP8.5 and blue for 2081-2100 under RCP8.5_FixA. (**e-h**) are identical to (**a-d**), except for that (**e-h**) are calculated after the long-term temperature trend has been removed from the raw dataset. The results are shown for the global land (GLO), Australia (AUS), Brazil (BRA), China (CHA), Europe (EUR), India (IND), Southern Africa (SAF), and contiguous USA (USA). Detailed calculation procedures of these values shown here are provided in **Text S5**.

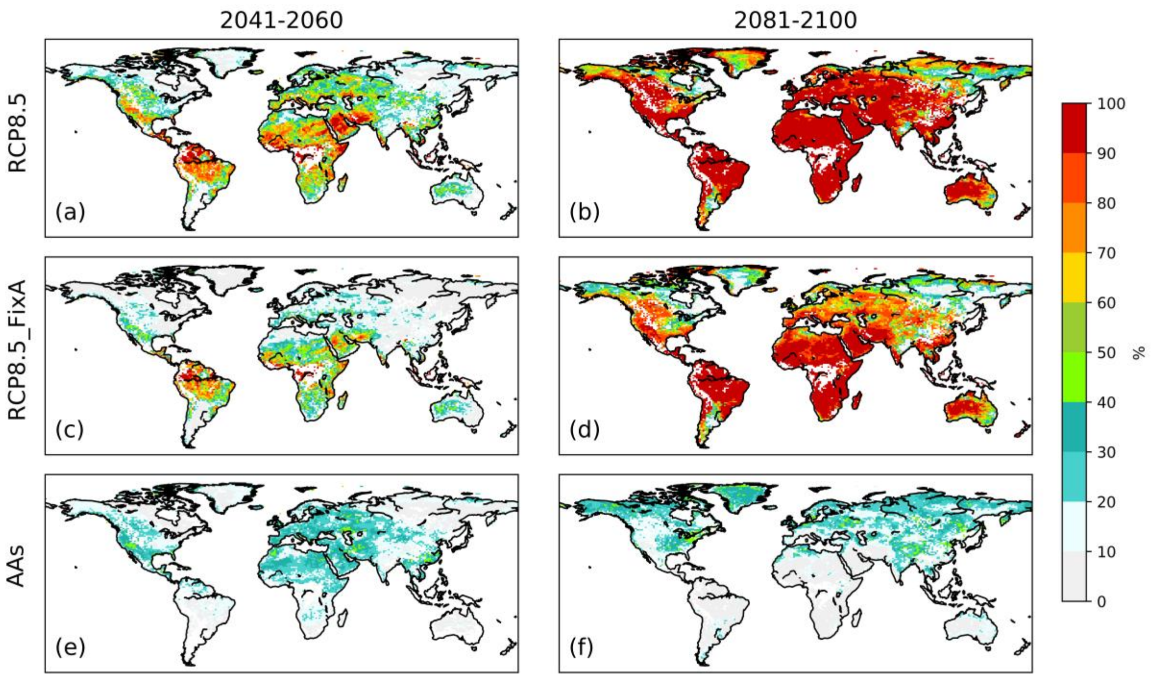

Figure 2 Exceedance probability of heatwave magnitude over 2041-2060 (left) and 2081-2100 (right) relative to the baseline period (1986-2005), as calculated from all the ensemble members under (**a,b**) RCP8.5 (greenhouse gas increases (GHG)+aerosol reductions (AAs)), (**c,d**) RCP8.5_FixA (GHGs only) and (**e.f**) the contribution from aerosols.

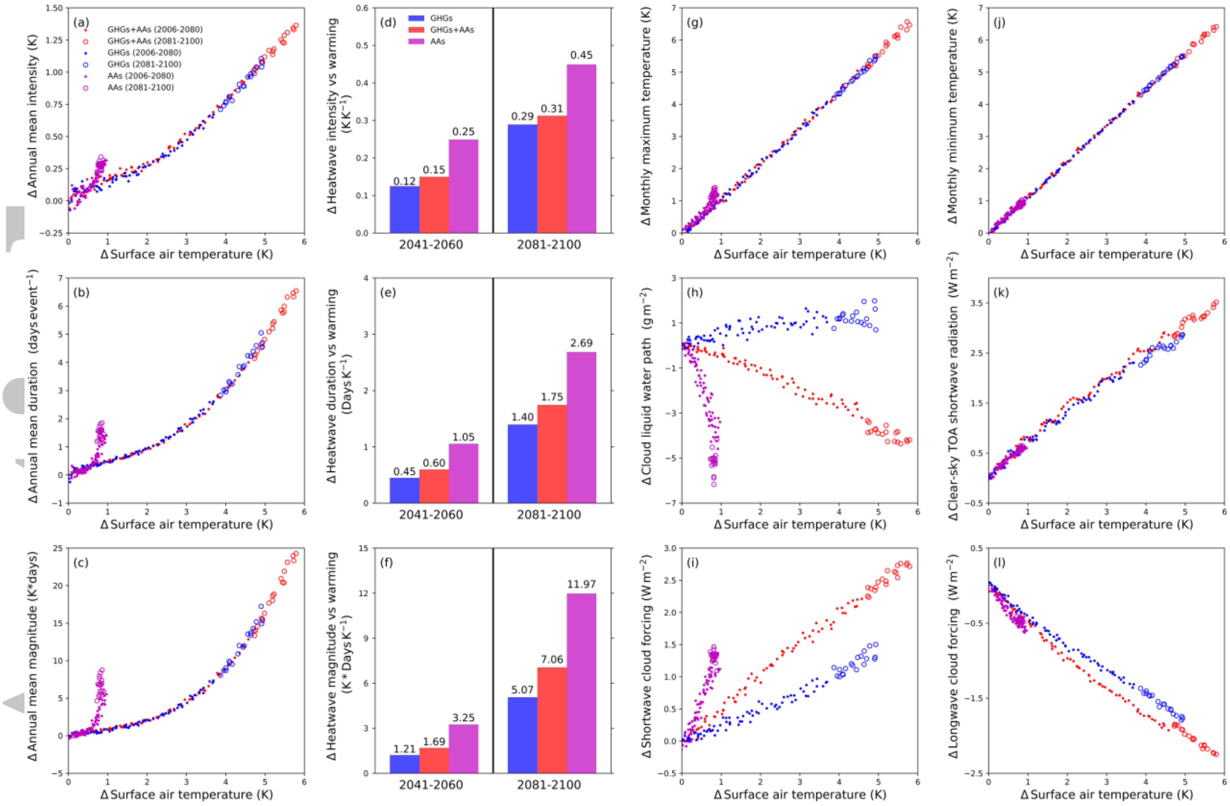

Figure 3 Sensitivity of heatwave metrics to warming: scatterplots of changes (ensemble mean of annual mean) in land area-weighted mean heatwave (**a**) intensity (K), (**b**) duration (days event^{-1}), and (**c**) magnitude (K*days) against global land mean surface temperature change. The sensitivity of changes in these metrics, derived as the slope of the linear fitting of the scatterplots in **a-c**, are shown in **d-f** for the time period 2041-2060 and 2081-2100, respectively. Also shown are changes in the annual mean of global area-weighted mean (**g**) monthly maximum temperature (TX, K), (**h**) cloud liquid water path (CLWP, g m^{-2}), (**i**) shortwave cloud forcing (SWCF, W m^{-2}), (**j**) monthly minimum temperature (TN, K), (**k**) clear-sky shortwave radiation at top-of-the-atmosphere (SWCST, W m^{-2}) and (**l**) longwave cloud forcing (LWCF, W m^{-2}), all plotted against land area-weighted mean surface temperature change (K). All scatterplots are plotted separately for the period 2006-2080 (filled small dots) and 2081-2100 (large circles). The colour conventions are: red for RCP8.5 (GHGs + AAs), blue for RCP8.5_FixA (GHGs only) and magenta for aerosols differentiated as RCP8.5 - RCP8.5_FixA.